Proceedings 10th NUMGE 2023
10th European Conference on Numerical Methods in Geotechnical Engineering
Zdravkovic L, Kontoe S, Taborda DMG, Tsiampousi A (eds)

https://doi.org/10.53243/NUMGE2023-89

Modelling of hydraulic fracturing based on element-scale fluid-solid coupling using multiple local coordinate system

Y. Wang, A.A. Javadi

Department of Engineering, University of Exeter, Exeter, UK

ABSTRACT: This paper presents the development and application of a new improved plain-strain numerical model for simulation of hydro-mechanical coupling in hydraulic fracturing using extended finite element method. The governing equation for fluid flow employs the Reynold's lubrication equation. In the computation of fluid velocity, the integration is dependent on the path of fluid flow and the direction of opening width of fracture. Using a uniform global coordinate system, it is difficult to deal with continuous changes in direction of fluid velocity as fracture propagates. To address this problem, a multiple local coordinate system is proposed to promote computation. In this system, each fracture segment is approximated as a liner equation; the origin of the local coordinates is set at the intersection point of two segments, and flow path of fluid is set along the direction of segment extension. Each local coordinate system is independent of the other local coordinate systems and the global coordinate system. By multiple local coordinate system, a new fluid-solid coupling method at element scale is introduced to enhance the accuracy of numerical solution. The developed model is verified against an analytical solution. This method can be used for modelling of more complex hydraulic fracturing morphologies.

Keywords: Hydraulic fracturing; coupling; fluid element; solid element

1 INTRODUCTION

Hydraulic fracturing has become an effective stimulation method to improve the productivity of formation, especially for unconventional resources (Economides and Martin, 2007). Many hydraulic fracturing methods have been developed in the past century, contributing to the considerable exploitation of oil/gas stored in deep reservoirs (Valkó and Economides, 1995). In order to study hydraulic fracturing, a series of hydraulic fracturing models have been developed to predict fracture evolution. In terms of 2D hydraulic fracturing in plain strain condition, PKN (Perkins and Kern, 1961; Nordgren, 1972) and KGD models (Geertsma and De Klerk, 1969) have been proposed to provide recommendable design schemes for certain formations, facilitating the treatment process in the wellbore. With further development of hydraulic fracturing, more complex morphologies have emerged in the stimulation treatment, posing more challenges to investigation by analytical methods. To overcome this difficulty, numerical simulation is increasingly popular and cost-efficient, and has been commonly used by many researchers in contrast to laboratory testing (Bakhshi et al., 2021; Fatahi et al., 2016). This paper will use extended finite element method (XFEM) to study hydraulic fracturing (Lecampion, 2009; Gordeliy and Peirce, 2013) and relative solid-fluid coupling process. XFEM has advantages in modelling crack propagation due to its characteristic of avoiding mesh refinement and remeshing as crack propagates, leading to large savings in computational efforts (Moës, 1999). It can model arbitrary propagation of crack, independent of mesh, without pre-setting crack path (Zhuang, 2014). The application of XFEM is an efficient way to model hydraulic fracturing and shows a promising prospect in providing a decent design plan and promoting the exploration of underground resources.

Based on XFEM, a multiple local coordinate system is proposed to study the fracture propagation that is not aligned with global axes, thus improving the integral accuracy and promoting convergence. In addition, an element-scale fluid-solid coupling is introduced to enhance coupling effect between fluid flow and rock matrix. The research presented in this paper can provide useful information for more complex numerical simulations of hydraulic fracturing.

2 GOVERNING EQUATIONS FOR ROCK AND FLUID

To simplify the study, the fluid flow is regarded as a quasi-static process in different stages as crack propagates. The rock medium is considered isotropic, impervious and linear-elastic. The injection fluid is considered as incompressible Newtonian fluid with a constant viscosity and pumped into the initial fracture from one

point at wellbore. The fluid leak-off in tightly compacted rock is neglected because it has a slight effect on the entire model.

2.1 Governing equation for elastic medium

According to previous research (Moës, 2002), the weak form of governing equation for elastic medium is expressed as:

$$\int_{\Omega} \sigma : \epsilon(u) d\Omega = \int_{\Gamma_N} N \cdot u d\Gamma + \int_{\Gamma_t} (t^+ - t^-) \cdot u d\Gamma \tag{1}$$

where σ is stress tensor, ϵ is strain tensor, u is displacement, N is the pressure over the boundary Γ_N, t^+ and t^- are the normal tractions on positive and negative faces of the fracture Γ_t, respectively, Ω is the whole domain.

Equation (1) can be further simplified as

$$Ku = F \tag{2}$$

where K is stiffness matrix, F is external force.

In Equation (2), K can be obtained by XFEM (Belytschko, 1999), comprising of standard matrix, Heaviside enriched matrix and tip enriched matrix.

$$K_0 = \int_{\Omega} B_i^T D B_j d\Omega (i, j = s) \tag{3}$$

$$K_n = \int_{\Omega} B_i^T D B_j d\Omega (i, j = a, b) \tag{4}$$

$$K_{0,n} = \int_{\Omega} B_i^T D B_j d\Omega (i, j = s, a, b) \tag{5}$$

where B_s, B_a, B_b represent different strain differential operator matrices (standard, Heaviside enrichment and tip enrichment).

2.2 Governing equation for fluid flow

With reference to Yew et al. (1997) and considering the model in plain strain condition (Figure 1), Navier-Stokes equation can be simplified as

$$\frac{\partial p}{\partial x} = \mu \left(\frac{\partial^2 u_x}{\partial z^2} \right) \tag{6}$$

where p is fluid pressure, μ is fluid viscosity, u_x is fluid velocity in x-axis.

Considering the boundary conditions at the fracture surface (u_x=0 at z=±w/2; w is fracture opening width) and integrating Equation (6), one can have the volumetric flow rate q_s:

$$q_s = -\frac{w^3}{12\mu} \frac{\partial p}{\partial s} \tag{7}$$

where s, instead of x as a general expression, represents the path of crack propagation and fluid flow.

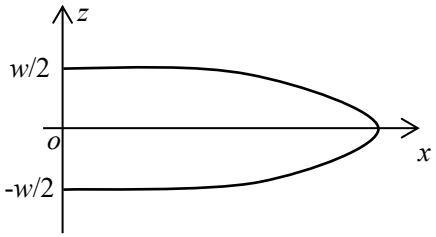

Figure 1. Plain strain model of hydraulic fracturing

By substituting Equation (7) into mass conservation equation, Reynold's governing equation can be derived as (Kirby, 2010; Currie, 2016):

$$\frac{\partial w}{\partial t} + \frac{1}{12\mu} \frac{\partial}{\partial s} \left(w^3 \frac{\partial p}{\partial s} \right) = Q_0 \delta(s) \tag{8}$$

where t is injection time, Q_0 is fluid volumetric source at the injection point, $\delta(s)$ is the Dirac delta function.

From the perspective of the whole domain in global coordinate system, Equation (7) is obtained by integrating Equation (6) over limits from -w/2 to w/2 with the integral variable z, which indicates the opening width w must be parallel to global z-axis (see Figure 1) as the fracture continuously propagates. So Equation (7) is only applicable for straight crack along global x-axis all the time. However, s in Equation (7) generally stands for arbitrary fracture path as fracture propagates, resulting in hydraulic fracture deviating off the global axis. Hence, the Equation (6) cannot be integrated for fracture propagation with varying deflection angle in fixed global coordinates.

To address this problem, in this paper a multi-phase local coordinate system is proposed to deal with fracture propagation that is not aligned with global axis. The multi-phase local coordinate system can create a framework of fracture segments in which the fracture opening width is always coincided with z-axis of local coordinates. This method can overcome the difficulty of irregular crack paths in fixed coordinate system, improving the accuracy of integral computation. Therefore, it can be used for more complex cases in modelling of hydraulic fracturing.

3 MULTI-PHASE LOCAL COORDINATE SYSTEM

The multi-phase local coordinate system developed in this research divides the crack path into several approximate linear sections, as shown in Figure 2. The length of crack growth in each step is defined as a fixed value. Each segment is located in a single local coordinate system where fluid flows through. For a single crack segment, a local coordinate system is built to keep the opening width of fracture parallel to the local z-axis within a certain range for integral calculation, and the

fracture propagation runs along the local *x*-axis. For two consecutive coordinate systems, the terminal point of the last segment will become the origin of the next local coordinate system. Note that the solution of rock deformation will still use global coordinate system. Generally, multi-phase local coordinate system is independent of mesh and global system, only dependent on the fracture path. So the whole system is featured in the form of a polyline along the crack segments and the fracture path is always perpendicular to the local *z*-axis. This formulation emphasizes the alternate use of two types of coordinate systems in modelling hydraulic fracturing: global coordinate system is used to deal with rock matrix; whereas local coordinate system is used to solve flow equation. The mathematical relationship of the two coordinate systems can be obtained by resorting to the intersection angle of axes and the locations of origins. The use of two coordinate systems can reduce the computational cost in calculating nodal coordinates, offering a good advantage over the use of a single (global) coordinate system.

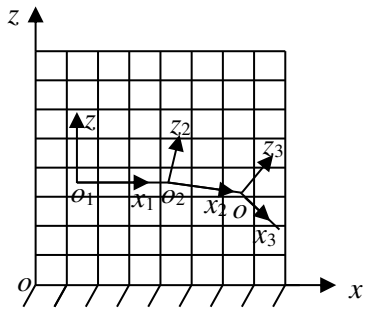

Figure 2. Multi-phase local coordinate system

For the sake of simplicity, it is assumed that the fluid element is one dimensional in the direction of flow, which is perpendicular to the direction of fracture opening. In a discretised fluid model, a single crack segment is meshed into several elements and each element includes two nodes at two extremities. The local coordinates of those nodes are calculated in accordance with their locations in fluid meshes. Next step is to obtain the global coordinates of those nodes for applying corresponding pressure on rock matrix. Thus, each crack segment is settled on two coordinate systems and the entire fluid flow equation can be expressed as:

$$q_{sum} = \sum_i^{Nseg} q_{s_i} = -\sum_i^{Nseg} \frac{w^3}{12\mu} \frac{\partial p}{\partial s_i} \tag{9}$$

where *Nseg* is the number of fracture segments.

In this research, a coupled hydraulic fracturing model is built to improve the accuracy of computation and to promote convergence. So the interaction of the two media plays an important role in the study of coupling and crack propagation. To strengthen the coupling effect, the interaction of the two media is simulated by a more accurate approach in the following section, involving the functions of variables transfer between the two media. Fluid pressure from each segment incorporated into elastic equation can be expressed as

$$K \sum_i^{Nseg} u_i = \sum_i^{Nseg} p_i \tag{10}$$

4 FLUID-SOLID COUPLING ALGORITHMS

The maximum opening width of fracture along the crack surface varies as the fracture propagates and the fluid is continuously injected into the borehole to promote fracture opening and propagation. The fracture fluid is discretized into one-dimensional linear elements along the crack path as the length of fluid flow is much greater than the opening width. To reduce the complexity of the calculations, fluid elements are assumed to have the same size as the edges of the square elastic elements. This implies that fluid elements only include the dimension in the flow direction and the width of fluid elements will be ignored. In most cases, fluid nodes cannot be located right on elastic nodes, so the two types of nodes are distributed in a staggered way. As shown in Figure 3, fluid nodes are randomly located inside several elastic elements, and the fluid elements and elastic elements have the same size *l*. The pressure along the fluid path is transformed into nodal forces to act on elastic nodes and the fracture opening width is calculated according to the nodal displacements on two sides of the fracture.

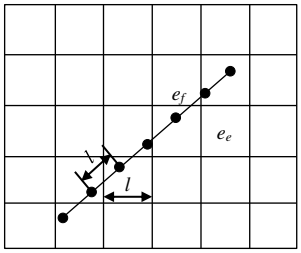

Figure 3. Distribution of two types of elements in one domain

4.1 Pressure transfer from fluid to rock

The first step of coupling process in hydraulic fracturing is to introduce an initial fluid pressure to apply on elastic body. The fluid pressure acting on two faces of the crack enhances the opening width of fracture. Since the fluid nodes and elastic nodes are distributed in a staggered way and do not necessarily coincide, it complicates the transfer of pressure from one medium to the other medium. If the mesh is fine, the distance between a fluid flow node and a corresponding elastic node in the direction normal to the crack is reasonably small, therefore the pressure value from fluid nodes can be directly ascribed to the elastic nodes. In this respect, finding the correspondence between nodes is an important step in order to gain a good accuracy of the solution. A

method based on the proximity of nodes is proposed by resorting to an example.

Now a rule regarding the pairing of corresponding nodes from these two media and application of fluid pressure to elastic body is demonstrated. First, an elastic node is used as a landmark, and the fluid node that has the shortest distance to this elastic node is regarded as the pairing node which applies stress to the landmark node. The process is explained in detail in Figure 4. A set of distances from an enriched node E (landmark) to its surrounding fluid nodes (A_1 A_2 A_3 A_4) are computed using nodal coordinates. This set of distances can be calculated as

$$D_i = \left\{\sqrt{(X_i - X_E)^2 + ((Y_i - Y_E)^2)}\right\}_{i=A_1,A_2,A_3,A_4} \tag{11}$$

The minimum value in the set can be selected. As it is shown, A_3 has the minimum distance to node E compared to the other three nodes, so A_3 is the pairing node of node E:

$$D_{min} = min(D_i) = D_{A_3} \tag{12}$$

The pressure on A_3 is assigned to node E. The pressure P_i is decomposed into two components along the x and y axes:

$$\begin{cases} p_{x_i} = p_i \cos\theta \\ p_{y_i} = p_i \sin\theta \end{cases} \tag{13}$$

where θ is the angle between the fracture segment and x.

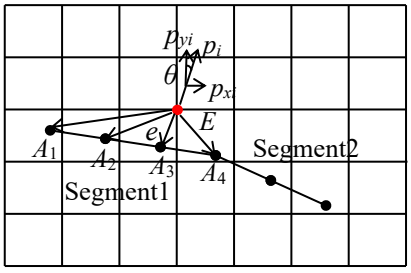

Figure 4. Pressure transfer from fluid nodes to elastic nodes

4.2 Evolution of fracture opening width

By applying the fluid pressure to the elastic body, Equation (10) is solved and the nodal displacement matrix is obtained. Based on nodal displacements, fracture opening width is derived by summing the offsets on the two faces of the fracture. So the opening width in Equation (8) can be approximately represented by the sum of the displacements on two elastic nodes on two sides of the crack if the mesh is fine. Four nodes of an elastic element are usually divided by the crack segment into two parts located on two sides of the segment. Each part is regarded as one set including different number of nodes (one, two or three nodes). From each set, a node with minimum distance to the fluid node is chosen as the target node and its displacement is considered as one-wing opening width of the fluid node.

In what follows the process of calculating the opening width is illustrated by an example for nodal displacements on two sides of fracture. In Figure 5, the fluid node F is located inside element e and the crack segment separates the four nodes to two sides of the fracture. Nodes A and B are considered as set A_1, and nodes C and D as set A_2. The distances from the four elastic nodes to the fluid node can be calculated by the equation:

$$d_i = \left\{\sqrt{(X_i - X_F)^2 + (Y_i - Y_F)^2}\right\}_{i=A,B,C,D} \tag{14}$$

By comparing the values of d_i it can be concluded that node B has the minimum distance to node F in set A_1 and node D has the minimum distance to node F in set A_2, so

$$min(d_{A1}) = d_B \tag{15}$$

$$min(d_{A2}) = d_D \tag{16}$$

Thus, nodes B and D are used as the target nodes on two wings of fracture to calculate total opening width; the opening width on node B is assigned to fluid node F as upward opening and the other opening width on node D is used as downward opening. The sum of the opening widths in two opposite directions is considered as the overall opening width on node F. As shown in Figure 5, d_x and d_y are displacements on node B along x-axis and y-axis, and d_x can be decomposed into components d_{x_1}, d_{x_2} which are parallel and normal to the crack segment respectively,

$$\begin{cases} d_{x_1} = d_x \cos\theta \\ d_{x_2} = d_x \sin\theta \end{cases} \tag{17}$$

where θ is the angle between crack segment and x-axis. In the same way, d_y can be decomposed into d_{y_1} and d_{y_2}:

$$\begin{cases} d_{y_1} = d_y \sin\theta \\ d_{y_2} = d_y \cos\theta \end{cases} \tag{18}$$

So one-wing opening width on node B is

$$d_1 = d_{x_2} + d_{y_2} \tag{19}$$

Similarly, the opening width on node D can also be obtained as

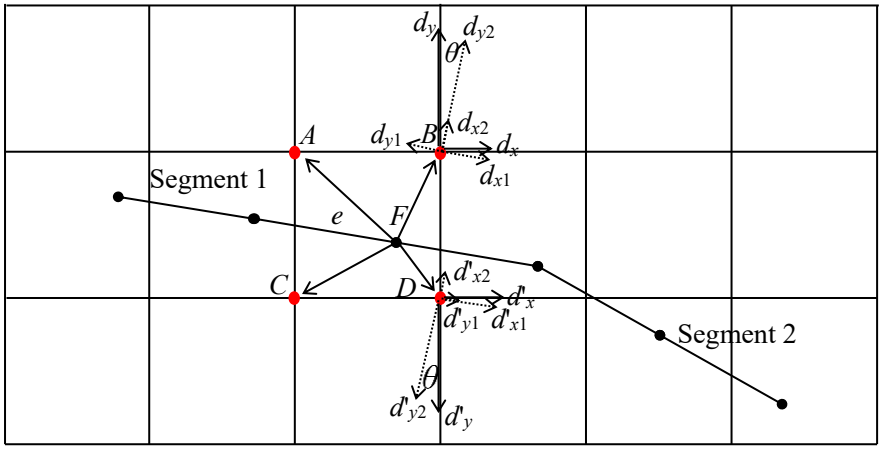

Figure 5. Sketch of calculation of fracture opening width

$$d_2 = d'_{y_2} - d'_{x_2} \tag{20}$$

The total width at node F can be expressed as

$$W_F = d_1 + d_2 = d_x \sin\theta + d_y \cos\theta + d'_y \cos\theta - d'_x \sin\theta \tag{21}$$

As frac-fluid with high pressure is continuously injected into a fracture, the opening width of the fracture in the elastic medium will increase continuously with time. Subsequently, it will be followed by a drop in the fluid pressure, which will in turn influence the pressure acting on the rock. The pressure drop is closely related to opening width and the flow length. Based on this rule, fluid flow and elastic body can be ideally coupled to investigate the fracture propagation and interaction effects. The basic coupling equations are as follows:

$$\begin{cases} K\sum_i^{Nseg} u_i = \sum_i^{Nseg} p_i \\ \frac{\partial w}{\partial t} + \frac{1}{12\mu}\frac{\partial}{\partial s}\left(w^3 \frac{\partial p}{\partial s}\right) = Q_0\delta(s) \end{cases} \tag{22}$$

in which displacement u, and fluid pressure p are two basic variables that connect the two equations. The proposed coupling algorithms can be used to solve equation (22).

5 VERIFICATION AND VALIDATION

In order to verify the effectiveness of the proposed methods, a coupled hydraulic fracturing model is set up based on our developed code and numerically simulated in comparison with the KGD analytical solution (Geertsma and De Klerk, 1969). The domain of the model has dimensions of 100m×100m and an initial horizontal fracture (5.5m) runs from the left edge (see Figure 6). The four boundaries are fixed along the directions normal to the edges (U_x=0 on left and right edges, U_y=0 on top and bottom edges). The rock parameters include elastic modulus (E=39.5GPa) and Poisson's ratio (v=0.3). The rock traction strength is 1e5Pa. The fluid injection rate is Q=0.00028m³/s, and its viscosity is 10mPa·s.

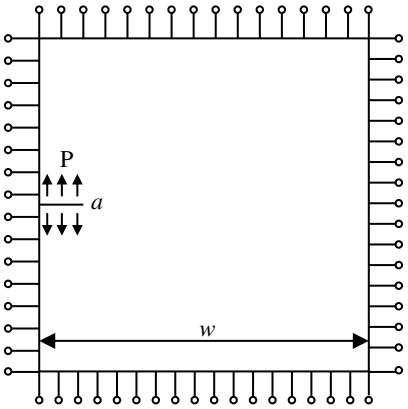

Figure 6. Sketch of fracture opening width along fluid nodes

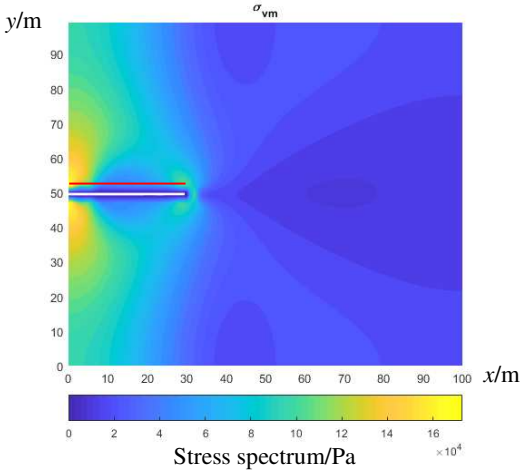

Figure 7. Sketch of fracture opening width along fluid nodes

The contour plot of the modelling result with the fracture propagated to 30m is shown in Figure 7 and the fracture basically keeps horizontal through the whole extension path as it propagates. In order to reflect the relation between the hydraulic fracture trajectory and the stress, a plot (Figure 8) was made according to the stress distribution along the red line in Figure 7. It can

be seen that the stress sharply decreases in the beginning stage and remains stable in the middle. When it is approaching the end stage, the stress starts rising again, which complies with the stress concentration at the tip. The comparison between the numerical solution and the analytical solution in terms of fracture half length against opening width is plotted in Figure 9. The result shows that the numerical solution is in a good agreement with analytical solution in the first half. However, the errors increase obviously in the later part, which can be caused by the increased fracture length (the increase of a/w). In contrast, the analytical solution of KGD model is assumed in an infinite domain.

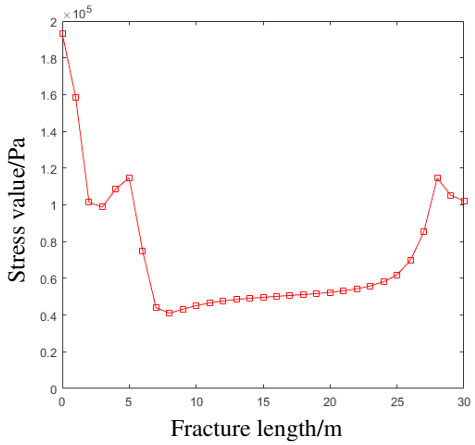

Figure 8. Stress variation along the fracture trajectory

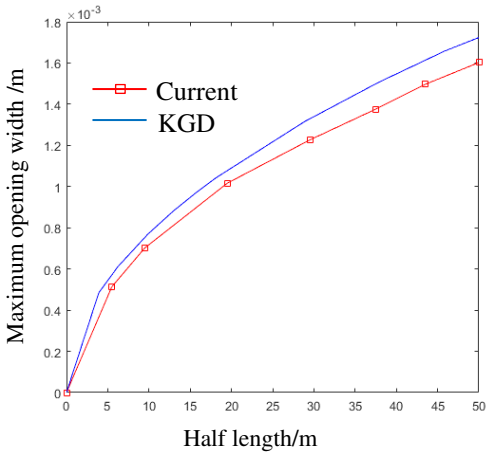

Figure 9. Comparison of numerical solution and analytical solution in terms of half length against opening width

6 CONCLUSION

This paper presented a multiple local coordinate system to deal with the changing direction of fluid flow in hydraulic fracturing when fracture propagates arbitrarily. It can promote convergence and reduce computation efforts. In addition, a strategy for solid-fluid coupling based on element size was proposed by analysing the interaction of two types of elements, which can improve the coupling effect and increase the accuracy of computation. These two algorithms were incorporated into XFEM to study evolution of hydraulic fracturing and the effectiveness was verified against analytical solution through an example. These findings can be used for the analysis of more complex hydraulic fracturing problems in the future.

7 REFERENCES

Bakhshi, E., Golsanami, N., Chen, L. 2021. Numerical modelling and lattice method for characterizing hydraulic fracture propagation: a review of the numerical, experimental, and field studies, *Archives of Computational Methods in Engineering* **28**(5), 3329-3360.

Belytschko, T., Black, T. 1999. Elastic crack growth in finite elements with minimal remeshing, *International Journal for Numerical Methods in Engineering* **45**(5), 601-620.

Currie, I.G. 2016. *Fundamental mechanics of fluids*, CRC press.

Economides, M.J., Martin, T. 2007. *Modern Fracturing: Enhancing Natural Gas Production*. ET Publishing, Houston, Texas.

Fatahi, H., Hossain, M.M., Fallahzadeh, S.H., Mostofi, M. 2016. Numerical simulation for the determination of hydraulic fracture initiation and breakdown pressure using distinct element method, *Journal of Natural Gas Science and Engineering* **33**, 1219-1232.

Geertsma, J., De, Klerk.F. 1969. A rapid method of predicting width and extent of hydraulically induced fractures, *Journal of Petroleum Technology* **21**(12): 1571-1581.

Gordeliy, E., Perice, A. 2013. Implicit level set schemes for modelling hydraulic fractures using the XFEM. *Computer Methods in Applied Mechanics and Engineering* **266**(1), 125-143.

Kirby, B.J. 2010. *Micro-and nanoscale fluid mechanics: transport in microfluidic devices*, Cambridge university press.

Lecampion, B. 2009. An extended finite element method for hydraulic fracture problems, *Communications in Numerical Methods in Engineering* **25**(2), 121-133.

Moës, N., Dolbow, J., Belytschko, T. 1999. A finite element method for crack growth without remeshing, *International Journal for Numerical Methods in Engineering* **46**(1), 131-150.

Moës, N., Belytschko, T. 2002. Extended finite element method for cohesive crack growth, *Engineering Fracture Mechanics* **69**(7), 813-833.

Nordgren, R.P. 1972. Propagation of a vertical hydraulic fracture, *Society of Petroleum Engineers Journal* **12**(4), 206-314.

Perkins, T., Kern, L.R., 1961. Widths of hydraulic fractures, *Journal of Petroleum Technology* **13**(09), 937-949.

Valkó, P., Economides, M.J., 1995. *Hydraulic fracture mechanics*, Wiley Chichester.

Yew, C., Weng, X.W. 1997. *Mechanics of Hydraulic Fracturing*, Gulf Pub, Co, Houston, TX.

Zhuang, Z., Liu, Z., Cheng, B., Liao, J., 2014. *Extended Finite Element Method*: Tsinghua University Press computational mechanics series, Academic Press.